

# Effect of Mobile Velocity on Communications in Fading Channels

Michael J. Chu, *Student Member, IEEE*, and Wayne E. Stark, *Fellow, IEEE*

**Abstract**—In a fading channel, it is well known that the rate of channel variation is dependent on the velocity of the mobile. Consequently, depending on the channel correlation, successive symbols transmitted over the channel can suffer from very similar or possibly very different fading conditions. In this paper, we present an analytical model to evaluate the effect of mobile velocity on the performance of a communication system operating in a multipath fading channel. To incorporate the effect of velocity, a Markov process is used which captures the correlated nature of the channel. An error recursion is then developed which considers the effect of closed-loop power control, channel coding, and finite interleaving. In the numerical analysis, we use the analytical model to investigate the tradeoffs when these various schemes are used. We demonstrate how the performance of these different schemes is sensitive to mobile velocity.

**Index Terms**—Error correction, fading channels, Markov processes, power control, time-varying channels.

## I. INTRODUCTION

WIRELESS communication systems suffer from a variety of channel impairments such as propagation loss, shadowing, multipath fading, and thermal noise. Fading has a particularly deleterious effect due to its time-varying nature and because deep fades in the signal amplitude lead to decoding errors at the receiver. Several techniques have been devised to counteract this type of channel impairment. However, because the correlation between fades is dependent on the speed of the mobile, the effectiveness of these schemes varies considerably as a function of mobile velocity.

In this paper, an analytical model is developed which characterizes the performance of a communication system in a fading channel as a function of mobile speed. A Markovian model for the fading channel is used that lends to a tractable analysis using finite-state channel (FSC) techniques. An error recursion is then developed which considers closed-loop power control, channel coding, and finite interleaving—common components in many communication systems. In particular, we show how the performance of these different schemes depends on the existing channel conditions. Moreover, the use of a combination of these schemes significantly improves the overall performance of the system.

There has been extensive analysis of the performance of communication systems over a fading channel. Much of this research considers independent fading between symbols; the performance of coded communication systems over fading chan-

nels with perfect interleaving is reviewed in [1]. Early work done with FSC's is reviewed in [2]. In [3], the performance of Reed–Solomon (RS) codes is considered for the Fritchman channel model. The packet error rate in a noninterleaved fading channel is studied using error recursions in [4]. In [5], the performance of coded communications over a FSC with finite interleaving is considered. Two alternative methods of modeling multipath fading as a Markov process are considered in [6] and [7]. In [8] and [9], the effect of mobile velocity on the performance of various system models is considered through simulation.

The organization of this paper is as follows. In Section II, we introduce the system model and state various basic assumptions. The characterization of the fading channel as a Markov process is then discussed in Section III. In Section IV, the model used for closed-loop power control is reviewed. Section V presents analysis used to derive the performance of the system with FSC techniques. The effects of power control, coding, and interleaving are considered. Numerical results and discussion are presented in Section VI. Finally, Section VII summarizes results and presents conclusions.

## II. SYSTEM AND CHANNEL MODEL

A communication system using binary phase shift keying (BPSK) modulation is considered. The mobile user's data bit stream  $b_n$  is modeled as a sequence of mutually independent binary random variables, each with probability 1/2 of being +1 or -1. The resulting baseband model of the transmitted waveform for the BPSK signal with rate  $R = 1/T$  is given by

$$s(t) = \sqrt{\frac{2}{T}} \sum_{n=-\infty}^{\infty} b_n l_n p_T(t - nT) \quad (1)$$

where  $p_T(t)$  is a unit amplitude pulse in the interval  $[0, T]$  and  $l_n$  is the correction factor due to closed-loop power control. The power control model will be considered in more detail later.

The transmitted signal is corrupted by multipath fading and additive white Gaussian noise. By using a narrowband system model, the multipath fading is accurately modeled as a frequency nonselective time-varying multiplicative distortion with some phase shift. At the receiver, we assume that the phase can be perfectly estimated. Thus, with coherent reception, the effect from fading is only due to the multiplicative effect. The input to the receiver is then given by

$$r(t) = a(t)s(t) + n(t) \quad (2)$$

where  $a(t)$  is a Rayleigh random process and  $n(t)$  is additive white Gaussian noise with two-sided spectral density  $N_0/2$ . It

Manuscript received June 17, 1998; revised December 3, 1998.

The authors are with the Department of Electrical Engineering and Computer Science, University of Michigan, Ann Arbor, MI 48105 USA.

Publisher Item Identifier S 0018-9545(00)00910-5.

is assumed that the fading stays constant over the entire bit duration, hence,  $a(t) = a_n$  for  $(n-1)T \leq t < nT$ . After the received signal is passed through an appropriately normalized matched filter, the output of the receiver is

$$Z_n = a_n l_n b_n + \eta_n$$

where  $\eta_n$  is the matched filter output due to thermal noise with variance  $N_0/2$ . If  $Z_n$  is greater than 0 the receiver demodulates bit  $b_n$  to be +1, otherwise, the bit is demodulated to be -1.

### III. CHARACTERIZATION OF THE CHANNEL

To make the analysis tractable,  $a(t)$  is modeled as a first-order Markov process. The Gaussian wide sense stationary uncorrelated scattering (GWSSUS) model from [10] is used where the underlying components of the fading process,  $X_r(t)$  and  $X_i(t)$ , are modeled as independent zero-mean Gaussian processes. Hence, given  $a(t)e^{j\Theta(t)} = X_r(t) + jX_i(t)$  and  $E[X_r(t)X_r(t+\tau)] = E[X_i(t)X_i(t+\tau)] = R_X(\tau)$ , the autocorrelation function from [11]

$$R_X(\tau) = \sigma^2 J_0(2\pi f_m \tau) \quad (3)$$

is used where  $2\sigma^2$  is the mean square value of fading,  $J_0(\cdot)$  is the zeroth-order Bessel function, and  $f_m$  is the Doppler frequency given as  $f_m = v f_c / c$  where  $v$  is the speed of the mobile,  $f_c$  is the carrier frequency, and  $c$  is the speed of light. Clearly, mobile velocity affects the fading process  $a(t)$  through the autocorrelation function  $R_X(\tau)$ .

#### A. Steady-State Distribution

To characterize the fading channel as a Markov process, a steady-state distribution and a transition matrix are needed. The probability density function (pdf) of the Rayleigh-distributed fading factor  $a_n$  from (2) is

$$p_{a_n}(a) = \frac{a}{\sigma^2} \exp\left(-\frac{a^2}{2\sigma^2}\right), \quad \text{for } a \geq 0. \quad (4)$$

Because a loglinear power control model is used, the fading will be expressed in decibels. Hence, after normalizing  $a_n$  with respect to its root mean square value ( $y_n = a_n / \sqrt{2\sigma^2}$ ), a transformation into decibels gives ( $A_n = 20 \log_{10} y_n$ )

$$p_{A_n}(A) = \frac{10^{A/10}}{10 \log_{10} e} \exp\left(-10^{A/10}\right). \quad (5)$$

To compute the steady-state distribution, the fading process  $a_n$  is partitioned into  $L$  intervals ( $U_1, U_2, \dots, U_L$ ). It is straightforward to numerically compute the steady-state probability  $\underline{P}_A$  where the  $k$ th element is given by

$$P_A^{(k)} = \int_{U_k} p_{A_n}(x) dx. \quad (6)$$

#### B. Transition Matrix

To capture the change in the channel model due to varying mobile speed, a transition matrix is developed which utilizes the Gaussian nature of the underlying components of the fading

process. First, an expression for the pdf of the current state of the faded channel conditioned on a past fade is needed. By using the GWSSUS assumptions, a result from [12] can be used on the underlying Gaussian components to generate the transition matrix. The joint distribution of  $r$  and  $s$ , two levels of fading separated by some time  $\tau$ , is

$$\begin{aligned} p_{a(t), a(t-\tau)}(r, s) \\ = \frac{rs}{\sigma^4(1-\rho^2)} \exp\left(-\frac{r^2+s^2}{2\sigma^2(1-\rho^2)}\right) I_0\left(rs \frac{|\rho|}{\sigma^2(1-\rho^2)}\right) \end{aligned} \quad (7)$$

where  $\rho = R_X(\tau)/\sigma^2 = J_0(2\pi f_m \tau)$  and  $I_0(\cdot)$  is the zeroth-order modified Bessel function. Clearly, this joint pdf depends on the speed of the mobile through  $\rho$ . After normalizing and transforming (7) into decibel units, Bayes' rule is used with (5) to obtain the conditional pdf

$$\begin{aligned} p_{A(t)|A(t-\tau)}(s|r) \\ = \frac{10^{s/10}}{10(1-\rho^2) \log e} \exp\left(-\frac{10^{s/10} + \rho^2 10^{r/10}}{1-\rho^2}\right) \\ \cdot I_0\left[10^{(r+s)/20} \frac{2|\rho|}{1-\rho^2}\right]. \end{aligned} \quad (8)$$

The distribution of this conditional pdf depends on  $\rho$ , a function of  $\tau$ , where  $\tau$  is the time between two successive fades. Thus, we obtain the transition matrix  $\mathbf{P}$  for two successive fades by setting  $\tau = T$  and integrating the conditional pdf in (8) over the appropriate intervals

$$P_{a,b} = \int_{U_a} \int_{U_b} p_{A_n|A_{n-1}}(s|r) dr ds. \quad (9)$$

This formulation gives a transition matrix that describes how the fading changes from bit to bit. Hence, (6) and (9) model the fading as a finite-state Markov channel. Although the fading channel is not Markovian, applying this model lends to a more tractable analysis.

### IV. POWER CONTROL MODEL

With the transmitter, channel, and receiver appropriately defined, we now describe the model used for closed-loop power control. By using a first-order Markov process to model the fading channel, we constrain the *memory* of the channel so that the current fade is dependent only on the most recent fade. The same structure is employed in the power control model so that it only depends on the previous update.

In the numerical analysis, an  $(n, k)$  RS code generated over Galois field  $GF(2^q)$  is considered. Clearly, this analysis can also be applied to any linear block code. To simplify the notation here, we assume an  $(n, k)$  binary linear block code is used. We will then describe the changes necessary for the model to be used with RS codes. Let  $R_p$  be the rate of power control updates; that is every  $T_p = 1/R_p$  s, a new update is sent from the base station to the mobile to adjust its power. The number of bits transmitted between power control updates is denoted by  $M = T_p/T$ . Each set of  $M$  bits is represented by a power control group where  $i$  is the index associated with the  $i$ th power control group and  $j$  indexes the  $j$ th bit in the  $i$ th power control group

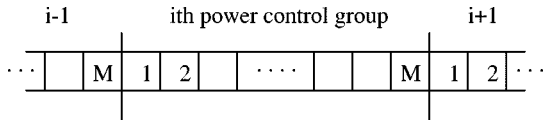


Fig. 1. Power control group.

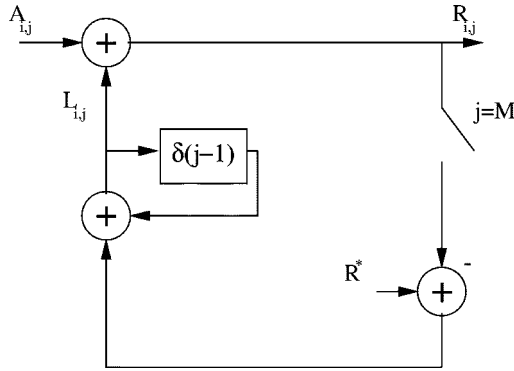


Fig. 2. Closed-loop power control.

where  $1 \leq j \leq M$ . Thus,  $a_n$ , the fading associated with the  $n$ th bit, is denoted by

$$a_{i,j} = a_n, \quad \text{when } n = iM + j.$$

This notation will be used interchangeably. A model of the separation of bits into power control groups is shown in Fig. 1.

In [13], a power control model was considered which transforms a standard closed-loop model into an analytically tractable loglinear model. A similar model is used in Fig. 2 that captures the essential points of the feedback loop. To impose linearity onto the entire loop the measurements are made in decibel units. Thus,  $l_n$ , the update computed by the power control loop in (1), is related to the transmitted power  $L_{i,j}$  by  $L_{i,j} = 20 \log_{10} l_n$  where  $n = iM + j$ .

In the figure,  $L_{i,j}$  is the transmitted power at the mobile and  $A_{i,j}$  is the loss due to Rayleigh fading. It is assumed that there is some open-loop power control mechanism that compensates for the channel loss from long-term effects such as shadowing and propagation loss.  $R_{i,j}$  is the received power at the base station where we assume that the base station can perfectly estimate the signal loss due to fading.  $R^*$  is some constant desired received power.

The power control loop updates the transmitter once after all  $M$  bits of a power control group are sent. In Fig. 2, when  $j = M$ , the last bit in the current power control group has been received. The switch then closes and the received power  $R_{i,M}$  of this last bit is compared to  $R^*$ , some preset desired power set by the base station. A correction factor is computed and sent back to the mobile. It is assumed that the correction factor is perfectly received by the mobile without delay. The correction factor is then combined with the previous transmitted power to form the new signaling power  $L_{i+1,1}$  for the next power control group. At all other times ( $j \neq M$ ), the switch stays open and the transmitted power does not change. Hence, immediately after the control loop updates the mobile, the first bits that are sent by the mobile will be able to counteract the loss from fading. However, as

the channel varies over time, the update from the power control loop will become outdated. How quickly the update becomes outdated will depend on the channel correlation which is a function of mobile velocity.

From this simple procedure, the received power  $R_{i,j}$  at the base station can be computed. The received power determines the signal amplitude and the ensuing performance of the communication system. When  $j = M$ , the last bit of the power control group is evaluated and a correction is sent to the transmitter. The transmitted power for the first bit of the new power control group is

$$L_{i,1} = L_{i-1,M} - R_{i-1,M} + R^*.$$

To obtain an expression for  $R_{i,j}$  for  $1 \leq j \leq M$ , we note that the received power of the first bit of the power control group is given by

$$\begin{aligned} R_{i,1} &= A_{i,1} + L_{i,1} \\ &= A_{i,1} + L_{i-1,M} - R_{i-1,M} + R^* \\ &= A_{i,1} - A_{i-1,M} + R^* \\ &= A_{i,1} - B_{i-1} + R^* \end{aligned} \quad (10)$$

where  $A_{i-1,M} = R_{i-1,M} - L_{i-1,M}$  and  $B_{i-1} \triangleq A_{i-1,M}$ . Thus, (10) gives an expression for the received power of the first bit in the  $i$ th power control group that is dependent only on the current fade, the previous fade, and some constant  $R^*$ . Since the transmitted power does not change within a power control group,  $L_{i-1,l} = L_{i-1,k} \forall l, k$ , then

$$R_{i,j} = A_{i,j} - B_{i-1} + R^* \quad (11)$$

for  $1 \leq j \leq M$ . Thus, we now have a general expression for the power control at the base station. The simple model does not approximate a typical feedback loop which usually averages over a series of measurements. However, it captures the essential points of closed-loop power control.

## V. SYSTEM PERFORMANCE

With the system appropriately defined, a closed form for the performance of the communication system as a function of mobile velocity is obtained. The performance of the system is considered when combinations of power control, coding, and finite interleaving are used. By modeling the fading channel as a first-order Markov process, we can develop an error recursion using FSC techniques that incorporates the time-varying nature of the fading process and considers the effect of coding and interleaving. Define  $P(m, n)$  as the probability of  $m$  errors in  $n$  bits. To compute the error recursion, two distinct cases need to be considered—a recursion for the coded bits within a power control group and an expression to relate the performance between separate power control groups.

### A. Error Recursion: Within a Power Control Group

Consider the  $i$ th power control group consisting of  $M$  bits. The value of the received power  $R_{i,j}$  in (11) depends on the update from the previous power control group  $B_{i-1}$ . The  $P(m, n)$

recursion can be computed by conditioning over the range of values that  $B_{i-1}$  can take on

$$P(m, n) = \sum_{l=1}^L P(m, n|B_{i-1} = U_l)P(B_{i-1} = U_l).$$

A recursion for the probability of  $m$  errors in  $n$  bits conditioned on  $B_{i-1}$  is obtained by partitioning the recursion over the quantized levels of fading ( $U_1, U_2, \dots, U_L$ ). This gives

$$P(m, n|B_{i-1}) = \sum_{l=1}^L P(m, n, A_{i,j} = U_l|B_{i-1})$$

where  $n = iM + j$  for  $1 \leq j \leq M$ . Letting  $P_l(m, n|B_{i-1}) \triangleq P(m, n, A_{i,j} = U_l|B_{i-1})$  to simplify notation, a recursion can now be obtained. The recursion for  $P_l(m, n|B_{i-1})$  is dependent on the terms  $P_l(m, n-1|B_{i-1})$  and  $P_l(m-1, n-1|B_{i-1})$  for all  $L$  states. Thus, the probability of  $m$  errors in  $n$  bits when the channel is in state  $U_k$  is

$$\begin{aligned} P_k(m, n|B_{i-1}) &= \sum_{l=1}^L P_l(m-1, n-1|B_{i-1}) \\ &\quad \cdot P(U_k|U_l)P(\xi|B_{i-1}, A_{i,j} = U_k) \\ &\quad + \sum_{l=1}^L P_l(m, n-1|B_{i-1}) \\ &\quad \cdot P(U_k|U_l)P(\bar{\xi}|B_{i-1}, A_{i,j} = U_k) \end{aligned} \quad (12)$$

where  $\xi$  is the event of an error for the  $n$ th bit. A proof of this expression can be found in the Appendix. Each summation in (12) consists of three terms  $P_l(\cdot, n-1|B_{i-1})$ ,  $P(U_k|U_l)$ , and  $P(\cdot|B_{i-1}, A_{i,j} = U_k)$ . The second term,  $P(U_k|U_l)$ , is given by the transition matrix from (9). The third term is the bit error probability where the received power at the base station given by (11) can be computed from the current level of fading  $A_{i,j} = U_k$  and the power control update  $B_{i-1}$  so that

$$P_{\text{bit error}} = Q\left(\sqrt{2 \cdot 10^{R_{i,j}/10}}\right). \quad (13)$$

Last,  $P_l(\cdot, n-1|B_{i-1})$  depends on the recursion itself and the initial values

$$\begin{aligned} P_k(0, 0) &= 1 \\ P_k(0, 1|B_{i-1}) &= P(\bar{\xi}|B_{i-1}, A_{0,1} = U_k)P(U_k|B_{i-1}) \\ P_k(1, 1|B_{i-1}) &= P(\xi|B_{i-1}, A_{0,1} = U_k)P(U_k|B_{i-1}) \\ P_k(m, n|B_{i-1}) &= 0, \quad \text{for } m < 0 \text{ and } m > n. \end{aligned}$$

In these initial terms,  $P(\cdot|B_{i-1}, A_{0,1} = U_k)$  is defined as in (13) and  $P(U_k|B_{i-1})$  is given by the transition matrix from (9). Thus, we have a recursion that applies to the bits within a single power control group.

### B. Error Recursion: Between Power Control Groups

In this section, a method is developed to compute the recursion between power control groups. Suppose in Fig. 3, the error recursion  $P(m, n)$  has been computed for all  $M$  bits in the  $i$ th power control group using the method described above. An expression is needed to relate the error distribution between power

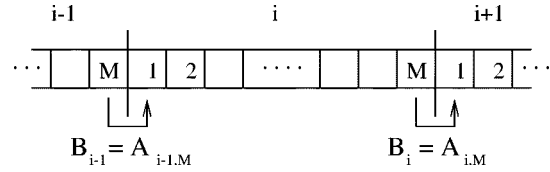


Fig. 3. Relating power control groups.

control groups  $i$  and  $i+1$ . Let  $P(m, N)$  where  $N = iM + M$  denote the error distribution for the very last bit of the  $i$ th power control group. From (12), we sum over all possible values of  $B_{i-1}$  to obtain

$$\begin{aligned} P(m, N, A_{i,M} = U_k) \\ = \sum_{l=1}^L P(m, N, A_{i,M} = U_k|B_{i-1} = U_l)P(B_{i-1} = U_l). \end{aligned} \quad (14)$$

Thus, we now have the probability of  $m$  errors in  $N$  bits when the current level of fading is  $U_k \forall k \in \{1, 2, \dots, L\}$  and  $\forall m \in \{0, 1, \dots, N\}$ . In our power control model, the value  $A_{i,M}$  is used as the update for the next power control group:  $B_i = A_{i,M}$ . Therefore, we can use  $A_{i,M}$  from (14) to feed the value of the new power control update  $B_i$  to the first bit of the  $(i+1)$ th power control group. The recursion for the first bit in the next power control group is

$$\begin{aligned} P(m, N+1, A_{i+1,1} = U_l|B_i = U_k) \\ = P(m, N|A_{i,M} = U_k)P(U_l|U_k) \\ \quad \cdot P(\bar{\xi}|B_i = U_k, A_{i+1,1} = U_l) \\ \quad + P(m-1, N|A_{i,M} = U_k)P(U_l|U_k) \\ \quad \cdot P(\xi|B_i = U_k, A_{i+1,1} = U_l). \end{aligned} \quad (15)$$

The proof is similar to the one found in the Appendix for (12). Thus, we now have a relation between the last bit in the  $i$ th power control group and the first bit in the  $(i+1)$ th power control group. To compute the rest of the bits in the power control group, we continue with the recursion described in the previous section.

### C. Interleaving

In this section, we describe how the effect of interleaving of the block-coded system is considered. An interleaver of depth  $d$  is used to separate successive bits from the same codeword by  $d$  bits from other codewords. With such an interleaver, we can modify the error recursion described above to account for the effect of finite interleaving. Since the modification is relatively straightforward, we will summarize the general procedure here.

After the bits are interleaved, they are combined into a succession of power control groups that are transmitted to the receiver. To compute the recursion, two distinct situations can occur. If two successive coded interleaved bits are in the same power control group, then (12) can be used to compute the recursion, however the transition  $P(U_k|U_l)$  is over  $d$  additional bits. For bits of the same codeword that are interleaved into separate power control groups, the recursion must be completed for the current power control group and then extended to the next group. Con-

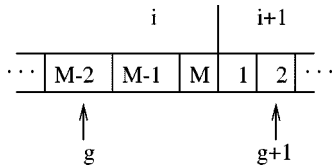


Fig. 4. Two interleaved bits in separate power control groups.

sider Fig. 4 where  $g$  and  $g+1$  are bits from the same codeword that are separated by  $d$  bits over two power control groups. To compute the error recursion, the error statistics for the  $i$ th power control group must be completed first. To do this, an equation similar to (12) is used where there are no errors

$$P_k(m, n|B_{i-1}) = \sum_{l=1}^L P_l(m, n|B_{i-1})P(U_k|U_l) \quad (16)$$

where  $P(U_k|U_l)$  is a transition from bit  $g$  to the last ( $M$ th) bit of the power control group. Then an equation similar to (15) can be used to relate the power control groups

$$\begin{aligned} P(m, n, A_{i+1,1} = U_l|B_i = U_k) \\ = P(m, n|A_{i,M} = U_k)P(U_l|U_k). \end{aligned} \quad (17)$$

Finally, (12) can be used to extend the recursion to bit  $g+1$  of the new power control group where the transition is from the first bit of the new power control group to the location of bit  $g+1$ .

#### D. Channel Coding

As mentioned earlier RS codes generated over  $GF(2^q)$  are used for error control in the numerical analysis. So far, we have presented a formulation for binary linear codes in order to simplify notation. To use RS codes, it is assumed that the fading stays constant over a symbol duration. Hence, the only modification necessary for the channel characterization is to let the transition matrix  $\mathbf{P}$  in (9) transition over a  $q$ -bit RS symbol so that  $\tau = qT$ .

Although the error recursion now counts  $P(m, n)$ , the probability of  $m$  errors in  $n$  symbols, the error recursion described above remains the same with the exception of (13). Instead of counting bit errors, now it is necessary to track symbol errors. Because it is assumed that fading stays constant over a  $q$ -bit symbol, the probability of symbol error can be computed from (13) using

$$P(\xi|B_{i-1}, A_{i,n} = U_k) = 1 - [1 - P_{\text{bit error}}]^q.$$

With the error recursion as defined which accounts for interleaving and power control, it is straightforward to obtain the performance of the communication system with coding. Given an  $(n, k)$  RS code with  $t$ -error correcting capability, the probability of packet error is given by

$$P_{\text{packet error}} = \sum_{m=t+1}^n P(m, n). \quad (18)$$

We now have an analytical model from which we can investigate the performance of a communication system as a function of velocity.

## VI. NUMERICAL RESULTS

In this section, numerical results are presented for the coherent reception of BPSK in the Markov-modeled Rayleigh fading channel. A  $(63, 33)$  RS code over  $GF(2^6)$  is considered where fading is quantized over 32 levels. The RS code is used because it is a nonbinary error correcting scheme that is ideally suited to bursty channels. The figures compare the packet error rate (PER) performance as a function of mobile speed when different combinations of power control, coding, and interleaving are considered. The plots are generated using  $R^*$ , the *desired* signal-to-noise ratio (SNR) for the receiver in (11). The unconventional use of  $R^*$  for SNR is due to the fact that when power control is used, the average received SNR changes as a function of mobile velocity. By considering  $R^*$ , a constant SNR expression can be used to compare the performance at different velocities.

Fig. 5 plots the packet error rate performance from (18) versus mobile velocity for a power controlled system at three levels of  $R^*$  with no channel coding. The carrier frequency used is  $f_c = 850$  MHz. There are  $M = 9$  RS blocks of uncoded bits per power control group. At low speeds, power control improves the performance significantly. This makes intuitive sense because at low speeds, the channel is highly correlated from symbol to symbol. When power control updates the transmitted power, it can effectively null out the signal degradation caused by multipath fading over many successive symbols because the fading varies slowly. However, as the velocity of the mobile increases, the performance of the power-controlled system worsens. As the rate of fading increases, the power control may work well for the first symbols of the power control group, but for subsequent symbols, since the fading changes rapidly, power control does not counteract the fading effect. At high velocities, this system is useless because there is virtually no correlation between successive symbols of a codeword.

Fig. 6 illustrates the PER performance of the coded system with *no* power control as a function of vehicular velocity. We see a much different relationship when coding is used. The best performance for the  $(63, 33)$  RS code is at high speeds. When the signal experiences a fast fading channel, successive symbols in a codeword will suffer from nearly uncorrelated fading. Hence, performance is best at high speeds because the RS code can correct intermittent symbol errors due to the channel. However, as the speed decreases, the performance worsens because the fading channel becomes more correlated. If a deep fade corrupts the codeword, the fade may lead to a burst of errors that surpasses the error correcting capability of the RS code.

From Figs. 5 and 6, we observe that power control and coding mitigate the effect of the faded channel at low speeds and high speeds. However, at intermediate speeds, neither scheme works particularly well. Power control works poorly because the channel conditions change too quickly for the feedback loop to track the fading. Channel coding also works poorly at intermediate speeds because the correlation of the channel leads to longer bursts of errors that surpass the error correcting capability of the code. We consider the use of coding and *finite* symbol interleaving to improve performance at intermediary speeds without further reducing the overall rate of the system. If

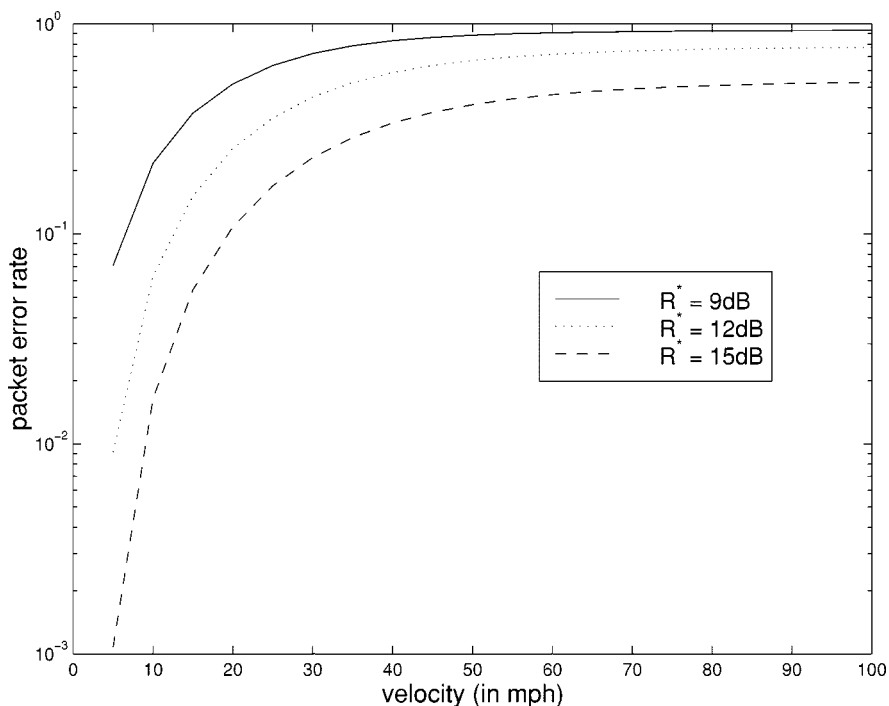


Fig. 5. Packet error performance as a function of velocity for three different values of  $R^*$ , the desired received SNR. A system employing closed-loop power control with no channel coding is used where nine uncoded blocks of bits are transmitted per power control group.

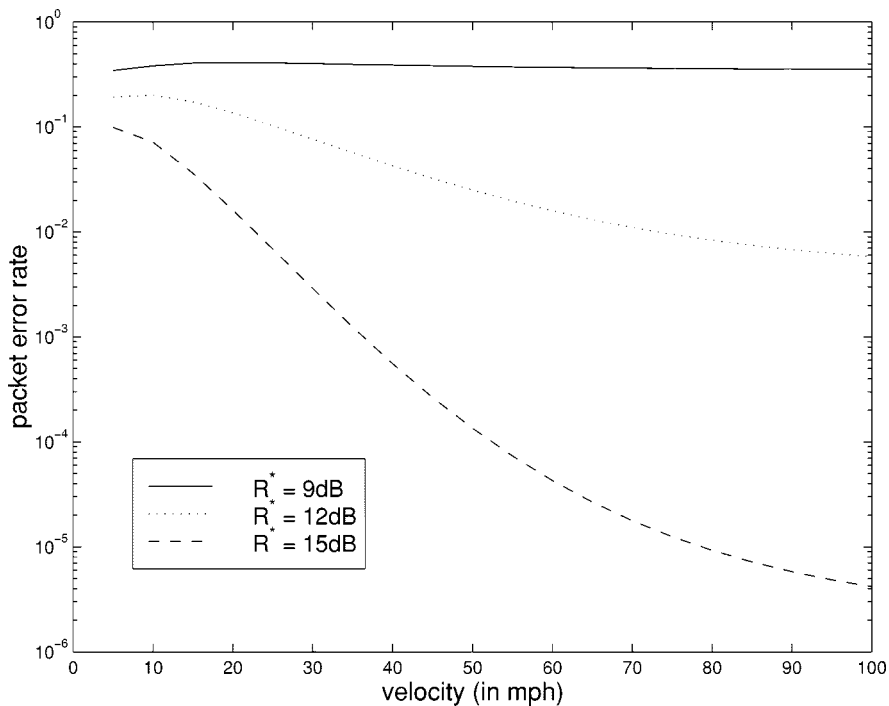


Fig. 6. Packet error performance as a function of velocity for a (63, 33) RS-coded system with no power control.

some delay can be tolerated, a combination of interleaving and coding can be used to improve the performance at intermediate speeds by breaking up the channel correlation between symbols of the same codeword. Fig. 7 plots the performance of the communication system when different interleaving depths are used with the (63, 33) RS code at a  $R^*$  of 12 dB. Clearly, the performance gain is at the intermediate speeds. Without

interleaving at these speeds, the system can experience deep fades that can surpass the error correcting capability of the RS code. With interleaving, the error bursts affect fewer symbols of the same codeword. Hence, the shorter bursts of errors that are experienced by the system with interleaving can be corrected by the RS code. At high speeds, the performance does not improve significantly because the fast fading channel

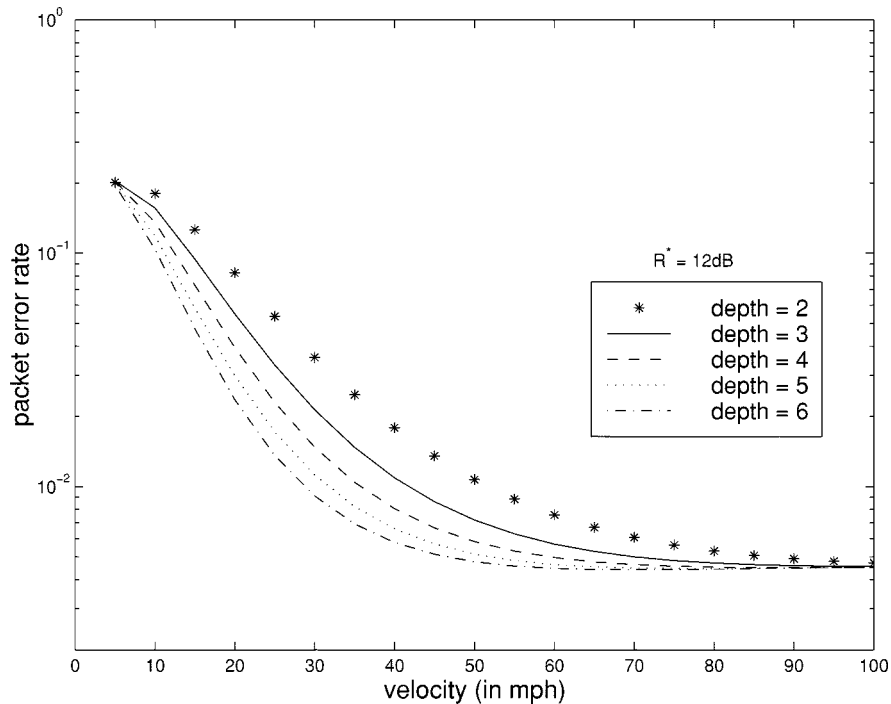


Fig. 7. Performance with (63, 33) RS coding when interleaving at various depths is used. No power control is considered and  $R^* = 12$  dB.

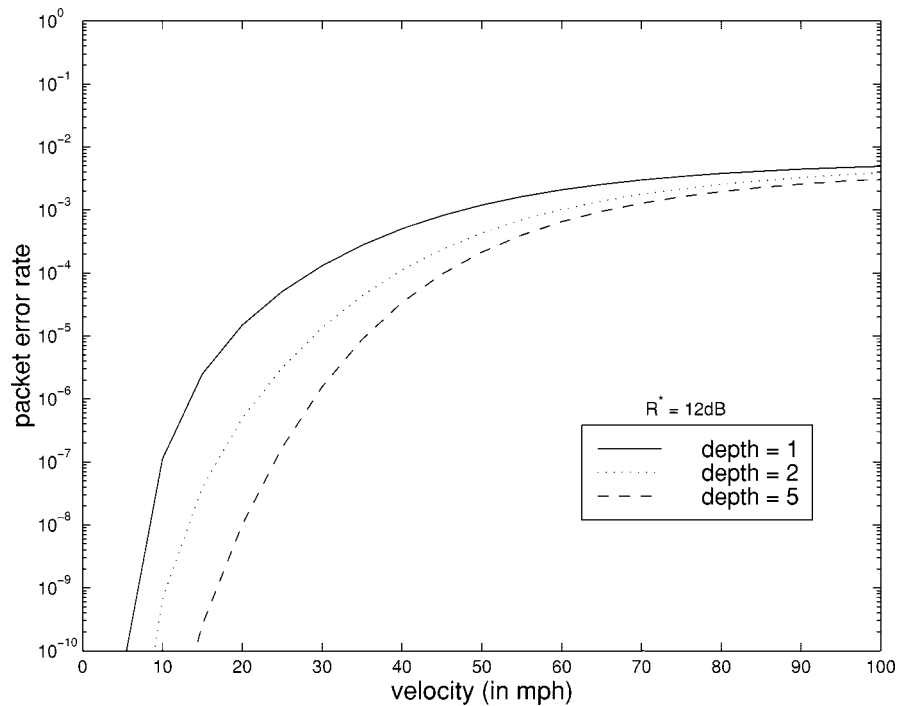


Fig. 8. Performance of combined system at various interleaving depths ( $R^* = 12$  dB). Each power control group consists of nine coded blocks.

“naturally” interleaves the codeword. At low speeds, finite interleaving does not give a performance gain because the error bursts are still too long.

From the figures above, we see that power control works well at low speeds while a combination of channel coding and interleaving works well at intermediate and high speeds. We would expect that combining power control, interleaving and coding would perform at least as well as the different schemes alone. Fig. 8 plots the performance of the combined system as a func-

tion of mobile velocity for a noninterleaved system and depths of two and five. The plots are obtained using a (63, 33) RS code at a  $R^*$  of 12 dB. The plot shows that the performance of the combined model over the entire range of velocities is considerably better than the performance of the individual components alone. We observe a significant improvement in performance at low speeds while the performance at high speeds approach those for the coding cases alone. This performance is due to the fact that coding can be used for any channel environment while

power control is only useful at low speeds. Because the channel is slowly varying at low speeds, the power control can track the fading very well and counteract it. After demodulation, the few errors due to this channel can than be corrected by the RS code. Hence, the good performance at low speeds. At high speeds, we only observe the gain due to coding. This is because power control is unable to track the fading at high speeds because the channel changes too quickly. We notice that interleaving helps the overall performance of the system with a significant gain at intermediate speeds. This is expected from the observations made earlier.

## VII. CONCLUSION

In this paper, we have presented a method to evaluate the performance of a communication system as a function of mobile velocity. Based on this model, we have investigated the performance of a communication system as a function of mobile velocity when power control, coding, and finite interleaving are considered. It has been shown that the correlation of the channel has a large influence on the performance of the overall system when these different schemes are considered. Moreover, a combination of these different techniques, can lead to an improvement in performance over a large range of velocities, that is, over the different channel conditions.

## APPENDIX

### DERIVATION OF THE ERROR RECURSION (12)

We would like to show that the following expression holds true:

$$\begin{aligned}
 P_k(m, n|B_{i-1}) & \quad (19) \\
 &= \sum_{l=1}^L P_l(m-1, n-1|B_{i-1}) \\
 & \quad \cdot P(U_k|U_l)P(\xi|B_{i-1}, A_{i,j} = U_k) \\
 &+ \sum_{l=1}^L P_l(m, n-1|B_{i-1})P(U_k|U_l) \\
 & \quad \cdot P(\bar{\xi}|B_{i-1}, A_{i,j} = U_k). \quad (20)
 \end{aligned}$$

Substituting the correct expression for the simplified notation in (19) and using total probability

$$\begin{aligned}
 P_k(m, n|B_{i-1}) & \\
 &= P(m, n, A_{i,j} = U_k|B_{i-1}) \\
 &= \sum_{l=1}^L P(m-1, n-1, \xi, A_{i,j-1} = U_l, A_{i,j} = U_k|B_{i-1}) \\
 &+ \sum_{l=1}^L P(m, n-1, \bar{\xi}, A_{i,j-1} = U_l, A_{i,j} = U_k|B_{i-1}) \quad (21)
 \end{aligned}$$

where the event  $\xi$  denotes that the  $n$ th bit was received in error. After simplifying the notation so that the event  $\beta \triangleq \{m-1$  errors in  $n-1$  bits}, we consider only the first term in (21)

$$\begin{aligned}
 & \sum_{l=1}^L P(\beta, \xi, A_{i,j-1} = U_l, A_{i,j} = U_k|B_{i-1}) \\
 &= \sum_{l=1}^L P(\beta, \xi, A_{i,j} = U_k|A_{i,j-1} = U_l, B_{i-1}) \\
 & \quad \cdot P(A_{i,j-1} = U_l|B_{i-1}) \quad (22)
 \end{aligned}$$

$$\begin{aligned}
 &= \sum_{l=1}^L P(\beta, \xi|A_{i,j} = U_k, A_{i,j-1} = U_l, B_{i-1}) \\
 & \quad \cdot P(U_k|U_l)P(A_{i,j-1} = U_l|B_{i-1}) \quad (23)
 \end{aligned}$$

where (22) and (23) are obtained by repeated uses of Bayes' Theorem where we replace  $P(A_{i,j} = U_k|A_{i,j-1} = U_l, B_{i-1})$  with  $P(U_k|U_l)$  in (23) because the fading process is Markovian. Using Bayes' theorem once more, we then find

$$\begin{aligned}
 & \sum_{l=1}^L P(\beta|\xi, A_{i,j} = U_k, A_{i,j-1} = U_l, B_{i-1})P(U_k|U_l) \\
 & \quad \cdot P(\xi|A_{i,j} = U_k, A_{i,j-1} = U_l, B_{i-1}) \\
 & \quad \cdot P(A_{i,j-1} = U_l|B_{i-1}) \\
 &= \sum_{l=1}^L P(\beta|A_{i,j-1} = U_l, B_{i-1})P(\xi|A_{i,j} = U_k, B_{i-1}) \\
 & \quad \cdot P(U_k|U_l)P(A_{i,j-1} = U_l|B_{i-1}) \\
 &= \sum_{l=1}^L P(\beta, A_{i,j-1} = U_l|B_{i-1})P(\xi|A_{i,j} = U_k, B_{i-1}) \\
 & \quad \cdot P(U_k|U_l) \quad (24)
 \end{aligned}$$

where in (24) the first term is simplified by noticing that  $\beta$ , the probability of  $m-1$  errors in  $n-1$  steps, does not depend on the future fade nor if the next bit is received in error. The simplification of the second term in (24) is due to the fact that the event  $\xi$  only depends on  $A_{i,j}$ , the current fade,  $B_{i-1}$ , the update from power control, and  $R^*$ , the desired SNR at the receiver. Finally, the last equation is obtained by combining terms through Bayes' rule again. Hence, we obtain the first term in (20). A similar proof holds for the second term of (20).

## REFERENCES

- [1] J. G. Proakis, *Digital Communications*. New York: McGraw-Hill, 1995.
- [2] L. N. Kanal and A. R. K. Sastry, "Models for channels with memory and their applications to error control," *Proc. IEEE*, vol. 66, pp. 724-744, July 1978.
- [3] A. I. Drukarev and K. P. Yiu, "Performance of error-correcting codes on channels with memory," *IEEE Trans. Commun.*, vol. COM-34, pp. 513-521, June 1986.
- [4] H. Bischl and E. Lutz, "Packet error rate in the noninterleaved Rayleigh channel," *IEEE Trans. Commun.*, vol. 43, pp. 1375-1382, Feb./Mar./Apr. 1995.
- [5] C. Pimentel and I. F. Blake, "Non-interleaved Reed-Solomon coding performance on finite state channels," in *IEEE Int. Conf. Communication*, vol. 3, 1997, pp. 1493-1497.



- [6] H. S. Wang and N. Moayeri, "Finite-state Markov channel—A useful model for radio communication channels," *IEEE Trans. Veh. Technol.*, vol. 44, pp. 163–171, Feb. 1995.
- [7] F. Swarts and H. C. Ferreira, "Markov characterization of channels with soft decision outputs," *IEEE Trans. Commun.*, vol. 41, pp. 678–682, May 1993.
- [8] A. Chockalingam and L. B. Milstein, "Closed-loop power control performance in a cellular CDMA system," in *29th Asilomar Conf. Signals, Systems and Computers*, vol. 1, Oct. 1996, pp. 362–366.
- [9] V. Weerackody, "Effect of mobile speed on the forward link of the DS-CDMA cellular system," in *Communication Theory Mini-Conf.*, 1995, pp. 147–151.
- [10] P. A. Bello, "Characterization of randomly time-variant linear channels," *IEEE Trans. Commun. Syst.*, vol. 11, pp. 360–393, Dec. 1963.
- [11] W. C. Lee, *Mobile Communications Engineering*. New York: McGraw-Hill, 1982.
- [12] K. Miller, *Multidimensional Gaussian Distributions*. New York: Wiley, 1964.
- [13] L. B. Milstein, A. Chockalingam, P. Dietrich, and R. R. Rao, "Performance of closed-loop power control in DS-CDMA cellular systems," *IEEE Trans. Veh. Technol.*, vol. 47, no. 3, pp. 774–789, 1998.



**Michael J. Chu** (S'97) received the B.S. degree in electrical engineering and computer science from the University of California at Berkeley in 1995 and the M.S. degree in electrical engineering and computer science from the University of Michigan, Ann Arbor, in 1997. He is currently working toward the Ph.D. degree in electrical engineering at the University of Michigan.

He has conducted research on wireless networks and mobile radios with the PATH lab at the University of California at Berkeley. He has also served as an intern at Science Applications International Corporation (SAIC). His research interests include spread-spectrum communications, channel coding, and communications theory.

Mr. Chu is a member of Eta Kappa Nu and Tau Beta Pi.



**Wayne E. Stark** (S'77–M'78–SM'94–F'98) received the B.S. (with highest honors), M.S., and Ph.D. degrees in electrical engineering from the University of Illinois, Urbana, in 1978, 1979, and 1982, respectively.

Since September 1982, he has been a faculty member in the Department of Electrical Engineering and Computer Science at the University of Michigan, Ann Arbor, where he is currently a Professor. He is also a Principal Investigator of an Army Research Office Multidisciplinary University Research

Initiative (MURI) project on low energy mobile communications. His research interests are in the areas of coding and communication theory, especially for spread-spectrum and wireless communication networks.

Dr. Stark was an Editor of *Communication Theory* for the IEEE TRANSACTIONS ON COMMUNICATIONS in the area of spread-spectrum communications from 1984 to 1989. He was involved in the planning and organization of the 1986 International Symposium on Information Theory which was held in Ann Arbor. He was selected by the National Science Foundation as a 1985 Presidential Young Investigator. He is a member of Eta Kappa Nu, Phi Kappa Phi, and Tau Beta Pi.